ANNALS of Faculty Engineering Hunedoara
– International Journal of Engineering
Tome XV [2017] – Fascicule 3 [August]

ISSN: 1584-2665 [print; online]
ISSN: 1584-2673 [CD-Rom; online]
a free-access multidisciplinary publication
of the Faculty of Engineering Hunedoara

[1.]A. CHARALAMBOS , [2.]M.A. OTHUMAN MYDIN

# CALCULATION APPROACHES FOR THIN-WALLED STEEL COMPONENTS AT AMBIENT TEMPERATURE

[1.]Department of Civil & Environmental Engineering, School of Engineering, University of Cyprus, Nicosia, CYPRUS
[2.]School of Housing, Building and Planning, Universiti Sains Malaysia, Penang, MALAYSIA

**Abstract**: As thin-walled cold-formed members are thin, this will give rise to behavioural phenomena, which are not usually encountered in the more familiar hot-rolled sections. Firstly, when thin-walled members are under compression, local buckling will occur since the plate width to thickness ratio is too high. One of the effects of local buckling is to reduce the member stiffness against overall flexure and torsion. Before local buckling occurs, the channel is under uniform compression and afterwards stress distribution in the channel is no longer uniform and load is mainly resisted by areas of high stiffness. Secondly, distortional buckling sometimes occurs in compressed lipped channel sections of intermediate length. Distortional buckling of a lipped channel usually involves rotation of the flanges and the lips around the flange-web junctions. Thirdly, cold-formed steel columns are more easily to fail in flexural buckling because they always have a larger slenderness compared to the same length of hot-rolled columns. Fourthly, since many cold-formed sections have either no, or only one, axis of symmetry, this means that these sections have a natural inclination to twist under load. Thus they will more easily fail in torsional buckling or flexural-torsional buckling. Finally, a cold-formed steel section may fail in shear buckling due to its small thickness. Therefore this paper focuses on calculation approaches for thin-walled cold-formed steel structures at room temperature.
**Keywords**: cold-formed, steel, thin-wall, ambient, structure, calculation method

## 1. INTRODUCTION

Cold-formed thin-walled steel members offer a high strength to weight ratio and are also easy to construct when compared to thicker hot-rolled steel members. Because of this, cold-formed thin-walled steel sections as load-bearing structural components, i.e. beams, floor joints, columns and load-bearing walls, are extensively used in low to medium-rise domestic and industrial buildings and in almost any imaginable location since it was first applied in building construction in about 1850 in the U.S.A. Its applications and our understanding of its behaviour have been further expanded in various fields by leaps and bounds since the first specification for cold-formed steel design was issued by the American Iron and Steel Institute (AISI) in 1946. Despite the availability of cold-formed steel framing, there are still basic barriers that impede its adoption in residential and industrial markets. Probably one of the primary barriers is that the building industry is generally reluctant to adopt alternative building methods and materials unless they exhibit clear quality or performance advantages. The fire performances of cold-formed structural members are important considerations when designing light weight steel building. However, reported studies of the fire performance of cold-formed thin-walled steel members are few and the behaviour of thin-walled steel structures in fire conditions is not clear. The design procedure for their fire protection is still largely based on the limited choices supplied by manufacturers on the basis of their standard fire resistance tests [1]. Not only is this expensive, but it also limits flexibility of the designer.

## 2. LOCAL BUCKLING

Local buckling is particularly prevalent in cold-formed thin-walled sections and is characterised by the relatively short buckling wavelength of individual plate elements. Two methods may be employed to deal with local buckling, one being a numerical method, such as the finite element method (FEM), the finite strip method (FSM) or the Generalized Beam Theory (GBT), the other being simple and empirical hand calculation equations. Numerical methods can be used to give very detailed information of local buckling stresses. But they are too complex and time consuming for daily design. In the hand analytical approach, a thin-walled steel section can be considered as composed of a number of plates joined together at mutual edges along which the conditions of continuity and equilibrium must be satisfied. Therefore, the problem of calculating the local buckling capacity of a member is transformed to the problem of calculating the local buckling capacity of the plate elements. For each plate, the local buckling capacity depends on the effective area of the plate, which is equal to the effective width of the plate multiplied by its thickness. The effective width of a plate depends on the stress distribution in the plate, the supporting condition and the width to thickness ratio of the plate.

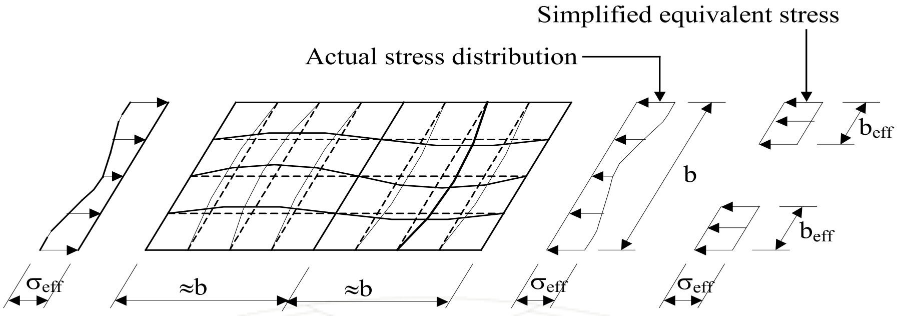


Figure 1. Effective width $b_{eff}$ of a plane element stiffened along both edges

Figure 1 illustrates the form of stress distribution usually encountered across the critical section of a uniformly compressed plate. The maximum stress occurs at the supported plate edges while stresses near the heavily buckled plate centre are relatively small, such that it can be considered that the effectiveness of the plate in withstanding loading is confined to the supported plate edges. The effective width concept assumes that the portions of a plate element (e.g. $b_{eff}/2$ in Figure 1) near the supports are fully effective in resisting load and the remainder of the element is completely ineffective as shown in Figure 1.

Winter's equation [2] is usually adopted by various design methods. It gives:

$$\frac{b_{eff}}{b} = 1 \qquad \text{if } \lambda \le 0.673 \tag{1}$$

$$\frac{b_{eff}}{b} = \frac{1}{\lambda}\left(1 - \frac{0.22}{\lambda}\right) \qquad \text{if } \lambda > 0.673 \tag{2}$$

in which the plate slenderness $\lambda$ is defined by:

$$\lambda = \sqrt{\frac{Y_s}{\sigma_{cr}}} = 1.052\frac{b}{t}\sqrt{\frac{Y_s}{Ek_\sigma}} \tag{3}$$

where, b is the plate width; $b_{eff}$ is the effective width of the plate; $\sigma_{cr}$ is the critical buckling stress of the plate, and $Y_s$ is the maximum edge stress of the plate and may be taken as the design yield stress of the plate. E is the Young's modulus; $k\sigma$ is a buckling factor, which is a function of the plate supporting condition. $k\sigma = 4.0$ for a simply supported plate in uniform compression and 0.43 for an outstand plate element with one edge free.

ENV 1993-1-3 (CEN 2001) made a small change in Eqn (1) and (2) for plate with different supports and also gives some comprehensive rules for determining the effective widths of a plate under different stress conditions by using Eqns (1) and (2). A slightly different approach to dealing with local buckling is adopted in the British standard (BS5950 Part 5 (BSI 1998)). The expression for effective width in BS5950 Part 5 is:

$$\frac{b_{eff}}{b} = [1 + 14(\sqrt{\frac{Y_s}{\sigma_{cr}}} - 0.35)^4]^{-0.2} \tag{4}$$

Due to a lack of test data, the AISI Specification (1996) treats unstiffened elements with stress gradients as if they were uniformly compressed under the maximum stress. Although BS5950 (BSI 1998) and ENV 1993-1-3 (CEN 2001) allow detailed calculations of the elastic buckling coefficient ($k\sigma$), the same effective width equation for a uniformly compressed element is used for elements with stress gradients.

**3. DISTORTIONAL BUCKLING**

Distortional buckling has only recently received the attention of researchers and a number of analytical methods have been developed for determining the elastic distortional buckling stress of singly

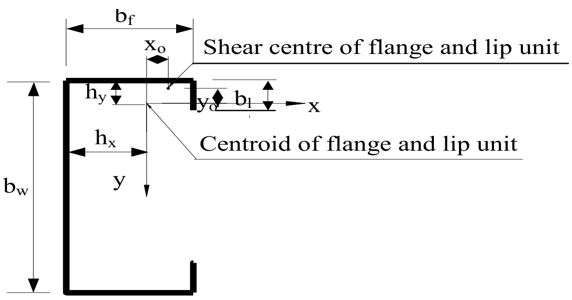

Figure 2. Cross-section of a lipped channel

symmetric cross-sections.

Refer to Figure 2, since distortional buckling mainly involves the rotation and lateral bending of the flanges, approximate expressions can be derived by considering the flanges in isolation, assuming that they are undistorted. The design formulas are given below:

$$P_{cr} = \frac{E}{2}\{(\alpha_1 + \alpha_2) \pm \sqrt{[(\alpha_1 + \alpha_2)^2 - 4\alpha_3]}\} \qquad (5)$$

where, $P_{cr}$ is the distortional buckling load.

$$\alpha_1 = \frac{\eta}{\beta_1}(\beta_2 + 0.039J\lambda^2) + \frac{K_\phi}{\beta_1 \eta E} \qquad (6)$$

$$\alpha_2 = \eta(I_y - 2y_0\frac{\beta_3}{\beta_1}) \qquad (7)$$

$$\alpha_3 = \eta(\alpha_1 I_y - \frac{\eta}{\beta_1}\beta_3^2) \qquad (8)$$

$$\beta_1 = h_x^2 + \frac{(I_x + I_y)}{A} \qquad (9)$$

$$\beta_2 = I_w + I_x(x_0 - h_x)^2 \qquad (10)$$

$$\beta_3 = I_{xy}(x_0 - h_x) \qquad (11)$$

$$\beta_4 = \beta_2 + (y_0 - h_y)[I_y(y_0 - h_y) - 2\beta_3] \qquad (12)$$

$$\lambda = \pi(\frac{E\beta_4 b_w}{2D})^{0.25} = 4.80(\frac{\beta_4 b_w}{t^3})^{0.25} \qquad (13)$$

$$\eta = (\frac{\pi}{\lambda})^2 \qquad (14)$$

$$K_\phi = \frac{Et^3}{5.46(b_w + 0.06\lambda)}[1 - \frac{1.11P'}{EAt^2}(\frac{b_w^2\lambda}{b_w^2 + \lambda^2})^2] \qquad (15)$$

P' is obtained with

$$\alpha_1 = \frac{\eta}{\beta_1}(\beta_2 + 0.039J\lambda^2) \qquad (16)$$

The distortional stress is

$$\sigma_{de} = \frac{P_{cr}}{A} \qquad (17)$$

In equations 5-17, E is the Young's modulus of steel; D is the lipped flange flexural rigidity, $D = \frac{Et^3}{12(1-\nu^2)}$; $\varpi$ is the Poisson's ratio; $I_x$ and $I_y$ are the second moments of area of the lipped flange about x, y axes, respectively; $I_{xy}$ is the product second moment of area of the lipped flange about the x, y axes; $I_w$ is the warping constant of the lipped flange; J is the torsion constant of the lipped flange; A is the cross-sectional area of the lipped flange; t is the thickness of the flange; $b_w$ is the depth of the web; $h_x$ and $h_y$ are the x, y coordinates of the flange/web junction; $x_0$ and $y_0$ are the x, y coordinates of the shear centre, as shown in Figure 2. In Figure 2, the origin of the x-y axes is at the centroid of the flange and lip unit. The formulations are:

$$\sigma_{max} = f_y(1 - \frac{f_y}{4\sigma_{de}}) \quad \text{if } \sigma_{de} \geq \frac{f_y}{2} \qquad (18)$$

$$\sigma_{max} = f_y\left[0.055\left(\sqrt{\frac{f_y}{4\sigma_{de}}} - 3.6\right)^2 + 0.237\right] \quad \text{if } \frac{f_y}{13} \leq \sigma_{de} \leq \frac{f_y}{2} \qquad (19)$$

where $\sigma_{de}$ is the elastic distortional buckling stress, given by $\sigma_{de}$ in equation 2.17, $f_y$ is the yield stress.

The second is a modification plate-strength curve and is based mainly on the plate-strength design approach as used for distortional buckling in the AISI specification when the lip is not adequate to fully support the flange. The formulation is given by:

$$\frac{b_{eff}}{b}=1,\quad \lambda \le 0.561 \tag{20}$$

$$\frac{b_{eff}}{b}=(\frac{\sigma_{de}}{f_y})^{0.6}(1-0.25(\frac{\sigma_{de}}{f_y})^{0.6}),\qquad \lambda \ge 0.561 \tag{21}$$

The distortional buckling slenderness is defined as:

$$\lambda=\sqrt{\frac{f_y}{\sigma_{de}}} \tag{22}$$

These two proposed design equations are consistent when predicting distortional buckling load, but the second one is easier to combine with current code design methods to predict the failure load for mixed local and distortional buckling model including the case where local buckling occurs before distortional buckling. The generalized Beam Theory (GBT), which has been pioneered by Professor R. Schardt and his colleagues at the University of Darmstadt in Germany, has become a useful tool to study distortional buckling of thin-walled columns. Separate and combined individual buckling modes can be associated with load components in GBT.

The basic equation of GBT is

$$E^kC^kV'''' - G^kD^kV'' + {}^kB^kV = {}^kq \tag{23}$$

in which the second-order effects are excluded. Ignoring the shear effect, the equation for mode 'k' is

$$E^kC^kV'''' - G^kD^kV'' + {}^kB^kV + \sum_i\sum_j {}^{ijk}k({}^iW{}^jV')' = {}^kq \tag{24}$$

Where k denotes mode k; ${}^kC$ is the generalized warping constant; ${}^kD$ is the generalized torsional constant and ${}^kB$ is the transverse bending stiffness. The generalized section properties depend only on the cross-section geometry. ${}^{ijk}k$ is a three dimensional array of second-order terms which takes account of the interactions between in-plane stresses in the faces and out-of-plane deformations. ${}^kV$ and ${}^kW$ are the generalized deformation and warping stress resultants in the $i^{th}$ mode, respectively. E and G are the modulus of elasticity and shear modulus. ${}^kq$ is the uniformly distributed load and n is the number of modes in the analysis. The critical stress ${}^iW$, can be obtained if ${}^kq$ is zero.

If assuming that the member will buckle in a half sine wave of wavelength λ, the critical stress for single-mode buckling, which is valid for buckling in any individual mode, is [3]:

$${}^{i,k}W=\frac{1}{{}^{ijk}k}\left(E^kC[\frac{\pi}{\lambda}]^2+G^kD+{}^kB[\frac{\lambda}{\pi}]^2\right) \tag{25}$$

As the wavelength is varied, the minimum critical stress result is:

$${}^{i,k}W=\frac{1}{{}^{ijk}k}(2\sqrt{E^kC^kB}+G^kD) \tag{26}$$

and the corresponding half-wavelength is

$${}^k\lambda=\pi(\frac{E^kC}{{}^kB})^{0.25} \tag{27}$$

From equations 25, 26 and 27 it can be seen that the distortional critical stress resultant for mode k is only dependant on the second-order coupling term ${}^{ikk}k$ when the load is applied in a different mode i and the half wavelength depends only on the cross-section properties ${}^kC$ and ${}^kB$ which are independent of the load. Rotational restraint stiffness $k_\phi$ in equation (15) may become negative with increasing depth of the web from equation (15) and if the web buckles earlier than the flange, this may result in a low prediction of the distortional buckling stress. Therefore, for this case, a simple buckling model where the rotational restraint between the flange and the web can be treated as zero can be established and the buckling stresses in the flange and web can be analysed separately. As the buckling load P' of the flange alone can be obtained with $k_\phi$ taken as zero in equation (15), the buckling stress of the web plate is:

$$\sigma_w=\frac{\pi^2D}{tb_w^4}\left(\frac{b_w^2+\lambda^2}{\lambda}\right)^2 \tag{28}$$

When the buckling stress in the web is smaller than that in the flange, there is some buckling interaction and the mean buckling stress can be calculated approximately by:

$$\sigma_{cr}=(2P'+\sigma_wb_wt)/A_g \tag{29}$$

where, $A_g$ is the area of whole cross-section.

In the AISI Specification (1996), the inability of the edge stiffener to prevent distortional buckling is taken into account by reducing the local buckling coefficient of the plate element supported by the stiffener to a value below 4.0. In this method, the buckling coefficient ($k_\sigma$) can be chosen from Table 1.

Table 1. Buckling coefficient k to consider distortional buckling effect

| | Buckling coefficient $k_\sigma$ | |
|---|---|---|
| | $0.25 < w/b_f \le 0.8$ | $w/b_f \le 0.25$ |
| $\frac{w}{t} \le \frac{S}{3}$ | 4 | |
| $\frac{S}{3} < \frac{w}{t} < S$ | $k_\sigma = (4.82 - \frac{5b_L}{w})(\frac{I_s}{I_a})^{0.5} + 0.43 \le 5.25 - \frac{5b_L}{w}$ | $k_\sigma = 3.57(\frac{I_s}{I_a})^{0.5} + 0.43 \le 4.0$ |
| $S \le \frac{w}{t}$ | $k_\sigma = (4.82 - \frac{5b_L}{w})(\frac{I_s}{I_a})^{1/3} + 0.43 \le 5.25 - \frac{5b_L}{w}$ | $k_\sigma = 3.57(\frac{I_s}{I_a})^{1/3} + 0.43 \le 4.0$ |

Note: $S = 1.28\sqrt{E/f_y}$; $I_a$ is second moment of area of stiffener;

$I_s = (d^3 t \sin^2\theta)/12$; w, $b_L$ can be seen in Figure 3.

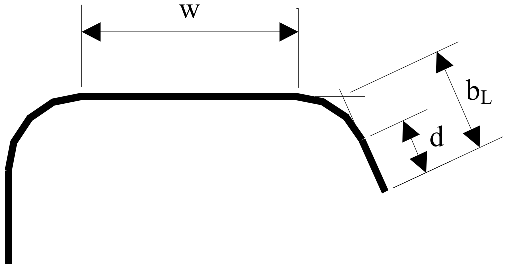

Figure 3. Elements with edge stiffener

The elastic foundation is represented by a spring whose stiffness depends upon the bending stiffness of the adjacent parts to the plate element of the cross-section under consideration and on the boundary condition of the element. The spring stiffness of the stiffener may be determined by applying a unit load per unit length to the cross-section at the location of the stiffener, as illustrated in Figure 4. The spring stiffness K per unit length may be determined form:

$$K = u/\delta \tag{30}$$

where $\delta$ is the deflection of the stiffener due to a unit load u acting in the centroid of $b_{e2}$ and $b_{eL}$. For an edge stiffener, the deflection can be obtained from;

$$\delta = \theta b_f + \frac{\mu b_f^3}{3} \times \frac{12(1-\nu^2)}{Et^3} \tag{31}$$

with $\theta = \mu b_f / C_\theta$

Therefore, the spring stiffness k can be stated as:

$$K = \frac{Et^3}{4(1-\nu^2)} \cdot \frac{1}{b_1^2 b_w + b_1^3 + 0.5 b_1 b_2 b_w k_f} \tag{32}$$

where, $b_1$, $b_2$ are the distance from the web-to-flange junction to the centre of the effective area of the edge stiffener of flange 1 and 2, respectively, as shown in Figure 4; $b_f$ is the flange width, $b_w$ is the web depth; $k_f = 0$ for a beam in bending, $k_f = \frac{A_{eff2}}{A_{eff1}}$ for a beam in axial compression, $k_f = 1$ for a symmetric beam.

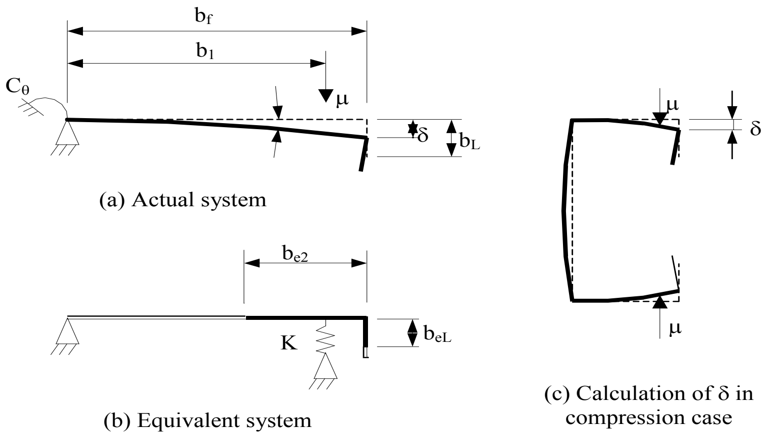

Figure 4. Determination of the spring stiffness K according to ENV1993-1-3 [4]

The critical buckling stress can be derived as:

$$\sigma_{cr} = \frac{2\sqrt{KEI_s}}{A_s} \tag{33}$$

in which, $A_s$ and $I_s$ are the effective cross-sectional area and the second moment of area of the stiffener, as shown in Figure 5. The rotational stiffness may be expressed as:

$$K_\phi = (K_{\phi f} + K_{\phi w})_e - (K_{\phi f} + K_{\phi w})_g = (K_{\phi f} + K_{\phi w})_e - f(\tilde{K}_{\phi f} + \overleftrightarrow{K}_{\phi w}) = 0 \tag{34}$$

Therefore, the critical buckling stress ($\sigma_{cr}$) is

$$\sigma_{cr} = \frac{(K_{\phi fe} + K_{\phi we})}{(\tilde{K}_{\phi f} + \overleftrightarrow{K}_{\phi w})} \tag{35}$$

where, $K_{\Box fe}$ and $K_{\Box fg}$ are the elastic rotational stiffness of the flange and the geometric rotational stiffness of the flange, repectively; $K_{\Box we}$ and $K_{\Box wg}$ are the elastic rotational stiffness of the web and the geometric rotational stiffness of the web, respectively [5]. Analytical models are needed for determining the rotational stiffness contributions from the flange and the web [6]. For the flange, cross-sectional distortion is not important; hence the flange is modelled as a column undergoing torsional-flexural buckling.

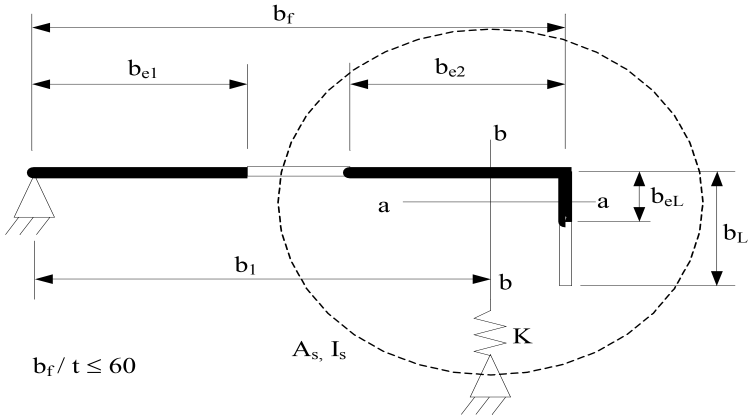

Figure 5. Effective cross-sectional area of an edge stiffener

For the web, cross-sectional distortion must be considered, so the web is modelled as a single finite strip. Therefore, the transverse shape function is a cubic polynomial [7]. The longitudinal shape functions of the flange and web are matched by using a single half-sine wave for each. The final rotational stiffness term for the flange and the web are presented as:

$$K_{\phi fe} = \left(\frac{\pi}{L}\right)^4 \left( EI_{xf}(x_{of} - h_{xf})^2 + EC_{wf} - E\frac{I_{xyf}^2}{I_{yf}}(x_{of} - h_{xf})^2 \right) + \left(\frac{\pi}{L}\right)^2 GJ_f \tag{36}$$

$$\tilde{k}_{\phi fg} = \left(\frac{\pi}{L}\right)^2 \left\{ A_f \left[ (x_{of} - h_{xf})^2 \left(\frac{I_{xyf}}{I_{yf}}\right)^2 - 2y_0(x_{of} - h_{xf})\left(\frac{I_{xyf}}{I_{yf}}\right) + h_{xf}^2 + y_{0f}^2 \right] + I_{xf} + I_{yf} \right\} \tag{37}$$

$$K_{\phi we} = \frac{Et^3}{6b_w(1-\nu^2)} \tag{38}$$

$$\tilde{k}_{\phi wg} = \left(\frac{\pi}{L}\right)^2 \frac{tb_w{}^3}{60} \tag{39}$$

The critical length can also be found and it is a function of the geometric terms. It can be calculated by:

$$L_{cr} = \left\{ \frac{6\pi^4 b_w(1-\nu^2)}{t^3} \left[ I_{xf}(x_{0f} - h_{xf})^2 + I_w - \frac{I_{xyf}^2}{I_{yf}}(x_{0f} - h_{xf})^2 \right] \right\} \tag{40}$$

where, E is elastic modulus; G is shear modulus; ν is poisson's ratio; t is the plate thickness; $b_w$ is the web width; L is the distance between restraints which limit rotation of the flange/web junction; $A_f$ is the gross area of the compression flange; $I_{xf}$ and $I_{yf}$ are the second moments of area of the flange along x and y direction, respectively; $I_w$ is warping constant of the flange. $x_{of}$ is x-distance from the flange/web junction to the centroid of the flange; $h_{xf}$ is x-distance from the centroid of the flange to the shear centre of flange, as shown in Figure 6.

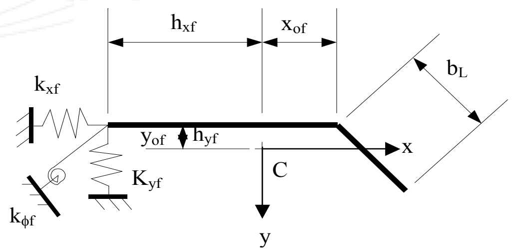

Figure 6. Flange model [6]

**4. GLOBAL BUCKLING**

For a thin-walled steel column under compression, the column may undergo different forms of global buckling, including flexural buckling, torsional buckling and combined flexural-torsional buckling. The local buckling and distortional buckling cause reduction in the effective stiffness of the member and thus affect the overall flexural and torsional-flexural buckling strength of the columns and lateral buckling strength of the beams [8]. Therefore, the ultimate failure of a thin-walled column under compression may be a combination of local and overall buckling or distortional and overall buckling. In design calculations, local and distortional bucking modes are considered first by evaluating the effective cross-section of the structural member. Global buckling is then checked using properties of the effective cross-section, which are obtained from local or distortional buckling behaviour. Due to local and distortional buckling, the centroid of the effective cross-section and the gross cross-section may not coincide. In this

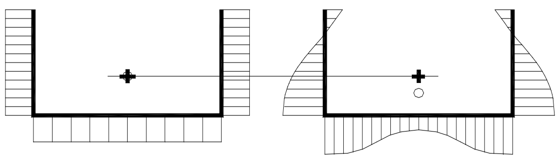
Figure 7. Neutral axis shift

situation, the effect of a shift in the centroid should be included, which can be seen in Figure 7. This shift in neutral axis is to introduce a bending moment in an axially loaded member. The shift results from the asymmetric redistribution of longitudinal stresses following the development of local buckling deformations, leading to an eccentricity of the applied load in pin-end columns.

In BS5950 Part 5, for sections symmetrical about both principal axes and closed cross-sections which are not subject to torsional flexural buckling, or are braced against twisting or columns with fixed end conditions, the flexural buckling load may be calculated as:

$$P_c = 0.5(\{P_{cs} + (1+\eta)P_E\} - [\{P_{cs} + (1+\eta)P_E\}^2 - 4P_{cs}P_E])^{1/2} \quad (41)$$

$$P_E = \frac{\pi^2 EI}{L_e^2} \quad (42)$$

$$\eta = 0.002(L_e / i - 20) \quad (43)$$

in which, $P_{cs}$ is the cross-sectional capacity for local buckling; I is the second moment of area of the cross section; $L_e$ is the effective length of the member; i is the radius of gyration of the gross cross-section corresponding to $P_E$.

For cross-sections with a single symmetry axis, the effects of movement of the effective neutral axis should be taken into account. The ultimate load carrying capacity for flexural buckling should be calculated as:

$$P_c' = \frac{M_c P_c}{(M_c + P_c e_s)} \quad (44)$$

where $M_c$ is the elastic bending moment capacity of the cross-section, $P_c$ is the flexural buckling capacity in which the neutral axis shit has not been considered and $e_s$ is the distance between the geometric neutral axis of the gross cross-section and that of the effective cross-section .

Different buckling curves, which should be chosen in accordance with the type of cross-section and axis of buckling, should be used to determine the flexural buckling capacity.

$$P_c = \chi A_{eff} f_y / \gamma_{M1} \quad (45)$$

$$A_{eff} = \Sigma t b_{eff} = \Sigma t \rho b = \beta_A A \quad (46)$$

$$\chi = \frac{1}{\phi + [\phi^2 - \overline{\lambda}^2]^{0.5}} \quad (47)$$

$$\overline{\lambda} = (\lambda / \lambda_1)[\beta_A]^{0.5} \quad (48)$$

$$\lambda = L_e / i \quad (49)$$

$$\lambda_1 = \pi[E / f_Y]^{0.5} \quad (50)$$

In AISI, the basic equation (51) can be used to determine the various global buckling load.

$$P_c = A_{eff} F_n \quad (51)$$

where, $F_n$ is determined as:

$$F_n = f_y(1 - f_y / 4F_e) \text{ for } F_e > f_y / 2 \text{ and } F_n = F_e \text{ for } F_e \le f_y / 2 \quad (52)$$

For flexural buckling, $F_e$ is

$$F_e = \frac{\pi^2 E}{(L_e / i)^2} = \frac{\pi^2 E}{(KL / i)^2} \quad (53)$$

where, $A_{eff}$ is the effective area of the cross-section and K is the effective length factor, which is related to the boundary condition.

If the cross-section of a column has only one axis of symmetry and without lateral bracing against twisting, the column may fail into torsional or torsional buckling mode. The load carrying capacity for torsional or torsional-flexural buckling in BS5950 Part 5 can be calculated as:

$$P_c = 0.5(\{P_{cs} + (1+\eta)P_{TF}\} - [\{P_{cs} + (1+\eta)P_{TF}\}^2 - 4P_{cs}P_{TF}]^{1/2} \quad (54)$$

$$P_{TF} = 0.5(\{P_{EX} + P_T\} - [\{P_{EX} + P_T\}^2 - 4\beta P_{EX} P_T]^{1/2} / \beta \quad (55)$$

$$P_{EX} = \frac{\pi^2 EI_X}{L_e^2} \quad (56)$$

$$P_T = \frac{1}{i_0^2}(GJ + 2\frac{\pi^2 EC_w}{L_e^2}) \quad (57)$$

$$\beta = 1 - (\frac{x_0}{i_0})^2 \quad (58)$$

$$i_0 = (i_x^2 + i_y^2 + x_0^2)^{0.5} \quad (59)$$

$$\eta = 0.002(\alpha L_e / i - 20) \quad (60)$$

$$\text{for } P_{EY} > P_{TF}, \quad \alpha = (\frac{P_{EY}}{P_{TF}})^{1/2} \quad (61)$$

$$\text{for } P_{EY} < P_{TF} \quad \alpha = 1 \quad (62)$$

in which, $I_x$ is the second moment of area about the x axis; G is the shear modulus; J is the St Venant torsion constant for the cross-section which may be taken as the summation of $bt^3/3$ for all element, where b is the element flat width and t is the thickness; $C_w$ is the warping constant for the cross-section; $x_0$ is the distance from the shear centre to the centroid measured along the x axis and $i_x$ and $i_y$ are the gyration about the x and y axes, respectively [9].

Buckling curve b is used to determine the torsional or torsional-flexural buckling capacities. The basic equation is the same as Eqn. 45, provided coefficient $\chi$ is decided as:

$$\chi = \frac{1}{\phi + [\phi^2 - \overline{\lambda}^2]^{0.5}} \quad (63)$$

$$\overline{\lambda} = (f_Y / \sigma_{cr})^{0.5} [\beta_A]^{0.5} \quad (64)$$

$$\sigma_{cr} = \sigma_{cr,TF}, \text{ but } \sigma_{cr} \le \sigma_{cr,T} \quad (65)$$

Based on 12 plain channel tests and 8 lipped channel tests, for studying coupled local and overall torsional-flexural buckling behaviour of cold-formed singly sysmemtric sections subjected to eccentric loads. They found that AISI and ENV1993-1-3 methods gave conservative predicted results [10].

**CONCLUSION**

Although the behaviour of cold-formed thin-walled steel structures at ambient temperature, including local buckling, distortional buckling, global buckling and shear buckling have been well understood and suitable design methods existed, there are only sporadic research studies of cold-formed thin-walled steel structures at high temperatures. Because of the lack of a systematic research study on cold-formed thin-walled steel structures in fire a suitable design procedure can not be drawn, which impedes the adoption of cold-formed thin-walled steel structures in the construction market.

**References**


[1] Gotluru BP. Torsion in thin-walled cold-formed steel beams. MS thesis, Cornell University, Ithaca, New York, 1998.

[2] Barsoum RS, Gallagher RH. Finite element analysis of torsional and torsional-flexural stability problems. International Journal for Numerical Methods in Engineering 1970;2(3):335–52.

[3] Rajasekaran S. Finite element method for plastic beam columns. In: Chen WF, Atsuta T, editors. Theory of Beam-Columns, vol. 2. New York: McGraw-Hill Inc, 1977:539–608.

[4] Attard MM. Lateral buckling analysis of beams by the FEM. Computers and Structures 1986;23(2):217–31.

[5] Attard MM, Somervaille IJ. Non-linear analysis of thin-walled open beams. Computers and Structures 1987;25(3):437–43.

[6] Chan SL, Kitipornchai S. Geometric nonlinear analysis of asymmetric thin-walled beam-columns. Engineering Structures 1987;9(4):243–54.

[7] Djugash ACR. Nonlinear biaxial bending behaviour of thin walled members. PhD thesis, Department of Civil Engineering, Indian Institute of Technology, Madras, India, 1988.

[8] Ellifrit D, Sputo T, Haynes J. Flexural strength and deflections of discretely braced cold formed steel channel and zee sections. Project report, American Iron and Steel Institute, 1991.

[9] Pi YL, Trahair NS. Nonlinear inelastic analysis of steel beam-columns. I: Theory. Journal of Structural Engineering, ASCE 1994;120(7):2041–61.

[10] Put BM, Pi Y-L, Trahair NS. Lateral buckling tests on cold-formed channel beams. Research report no. R767, Center for Advanced Structural Engineering, Department of Civil Engineering, The University of Sydney, Australia, 1998.